review

Analyzing protein functions in four dimensions

Janos Hajdu[1], Richard Neutze[1], Tove Sjögren[1], Karl Edman[1], Abraham Szöke[1], Rupert C. Wilmouth[2] and Carrie M. Wilmot[3]

Time-resolved structural studies on biomolecular function are coming of age. Focus has shifted from studies on 'systems of opportunities' to a more problem-oriented approach, addressing significant questions in biology and chemistry. An important step in this direction has been the use of physical and chemical trapping methods to capture and then freeze reaction intermediates in crystals. Subsequent monochromatic data collection at cryogenic temperatures can produce high resolution structures of otherwise elusive intermediates. The combination of diffraction methods with spectroscopic techniques provides a means to directly correlate electronic transitions with structural transitions in the sample, eliminating much of the guesswork from experiments. Studies on cytochrome P450, isopenicillin N synthase, cytochrome *cd*$_1$ nitrite reductase, copper amine oxidase and bacteriorhodopsin were selected as examples, and the results are discussed.

Biological function is a four-dimensional property, and a basic understanding of function requires a synthesis of knowledge in four dimensions (x, y, z; t). Time-resolved structural studies on biological macromolecules represent a necessary step in this direction. Here we review recent trends and results that indicate the maturing nature of this field, showing that an increasing variety of systems have yielded detailed mechanistic information on structural intermediates or unstable product complexes. We selected systems where time-resolved structural studies have led to genuinely new insights into our understanding of biological functions.

Three criteria[1–3] must be met to allow the study of structural changes of biological macromolecules in the crystalline state: (i) the macromolecule must be active in the crystal; (ii) a method of triggering the reaction within crystals must exist and should not disrupt the crystal lattice; and (iii) the structural intermediate of interest must be present at reasonably high concentration (preferably much above 25%) during data collection.

Reaction initiation in crystals

Recent time-resolved protein crystallographic studies fall into two main categories. One of these involves photon-induced reaction initiation followed either by monochromatic or Laue data collection, (see 'Data collection' section below). Photon triggering may involve the release of a caged substrate[3–5], may initiate a light sensitive reaction[6–16] or, when the photon trigger is X-rays, may reduce key groups through radiolysis[17]. Current developments in this area[6–15] represent an impressive technical achievement and map a pathway towards experiments in the picosecond to femtosecond regime[18–21]. It is difficult to trap structural intermediates that arise on these timescales; therefore, continuous pumping[6,9,12,14] and pump-probe methodologies[7,8,11] represent a promising avenue for structurally characterizing the fastest events in chemistry and biology.

Reaction triggering should ideally be both uniform throughout the body of the crystal and rapid with respect to the reaction under study. Very fast reaction initiation can be achieved by femtosecond photoexcitation[22], and in this time scale, even molecular vibrations are synchronized. On longer time scales, a transition into the Maxwell-Boltzmann regime occurs, and in this regime, chemical reactions do not proceed synchronously. Here, intermediates may be present simultaneously in many unit cells, but they are vibrationally uncoupled and thus unsynchronized. The interpretation of all time-resolved experiments is invariably compromized by this factor and by limitations in either the speed or uniformity of reaction initiation, partial occupancies, multiple conformational states, and crystal lattice disordering due to the very movements that one wishes to observe.

The majority of biochemical processes are not photochemical. Almost all enzymes participate in processes in which diffusion provides the link between reaction partners. Thus the second category of experiments targets these important processes and combines trapping methods with diffusion-based reaction initiation techniques[17,23–26]. Time-resolved structural studies on diffusive processes in enzyme crystals can be difficult due to problems of mixing enzymes and reactants. Structural studies are, however, possible on intermediates that accumulate transiently in the crystal during a reaction[1,27–29]. This requires a relatively fast substrate binding followed by a relatively slow reaction. Because the activity of an enzyme is generally lower in the crystalline state than in solution, uniform catalysis can often be triggered by diffusing reagents such as substrates into crystals. The rates of diffusion and ligand binding thus set an upper limit to the speed of reactions that can be analyzed this way. In an average-sized protein crystal (0.1–0.3 mm overall dimensions), half saturation binding with small ligands can be reached within about one minute. The turnover rate has to be slower than this to assure an accumulation of an intermediate. Intermediate trapping can be facilitated by using mutant proteins, altered substrates, changes in pH, pressure or temperature, or a combination of all these above. In cryo-trapping experiments, initial cooling rates of ~100,000 K s^{-1} can be reached on small crystals when immersed rapidly into liquid propane or ethane. This assures that the sample reaches cryogenic temperatures in a few milliseconds. With the availability of modern synchrotron sources, high quality monochromatic data collection on trapped intermediates is no longer an issue in such experiments.

[1]Department of Biochemistry, Uppsala University, Biomedical Center, Box 576, S-751 23 Uppsala, Sweden. [2]The Oxford Centre for Molecular Sciences and The Dyson Perrins Laboratory, South Parks Road, Oxford OX1 3QY, UK. [3]Astbury Centre for Structural Molecular Biology, School of Biochemistry and Molecular Biology, University of Leeds, Leeds, LS2 9JT, UK.

Correspondence should be addressed to J.H. *email: janos@xray.bmc.uu.se* or *C.M.W. email: c.m.wilmot@leeds.ac.uk*

Time-resolved experiments

It is important to distinguish time-resolved structural studies from time-resolved diffraction studies. In the latter, X-ray diffraction data are measured in real time, using either Laue diffraction[7,8,11,28–30] or fast monochromatic diffraction[23,27]. The difficulties of measuring changes in diffraction intensities in real time have made these types of experiments a specialty. Thus, an increasing number of studies attempt to trap intermediates at various stages of a reaction for subsequent data collection at cryogenic temperatures. This approach has produced a number of high quality structures for trapped intermediates (for examples, see refs 17,23–25), for which the reaction of interest was either slowed down appreciably or stopped entirely at a certain stage. Frames corresponding to various time points in the reaction can then be collected and assembled into a three-dimensional 'movie'[12,13,15,17,23–25]. Moreover, single crystal microspectrophotometry[4,23–25,29–32] provides a convenient way for establishing, in advance, conditions under which a high population of a desired structural intermediate builds up. Crystals with intermediates at different time points can be frozen, characterized in the home laboratory before a trip to a synchrotron for high resolution data collection.

Data collection

In time-resolved structural studies, multiple structural states are deliberately created in a crystal. A detailed analysis of mixed structures requires better quality and higher resolution diffraction data than those used in ordinary structure determinations. This requirement has been the main driving force in the application of monochromatic data collection methods for structural studies on transient reaction intermediates, and has also been driving the development of trapping methods to prolong the lifetime of otherwise short-lived intermediates.

During data collection with monochromatic X-rays, reflections are integrated through a small angular range. This diffraction geometry offers two advantages: it provides the highest attainable signal to noise ratios in intensity measurements (and thus the highest resolutions in the data set); and the geometry permits studies on crystals with high mosaicity. This point is important for measurements on reaction intermediates as a transient increase of disorder (and mosaicity) accompanies most structural transitions in crystals. A drawback of monochromatic data collection methods is the relatively slow speed of rotation photography, giving data rates of ~10,000 reflections per second presently.

In contrast, the Laue method employs a 'white' X-ray beam (typical $\Delta\lambda/\lambda$ values range from a few percent to over an octave) to illuminate a stationary crystal (for a recent review see ref. 33). Reflections are integrated through a small wavelength range instead of a small angular range. Under these conditions, a large number of lattice planes diffract simultaneously as the Bragg condition is satisfied for each of these planes by at least one narrow wavelength range in the spectrum. Extremely fast exposure can be achieved this way. Unfortunately, this method suffers from problems inherent to the geometry of Laue diffraction[2], and these features affect the usefulness of this method in time-resolved structural studies: (i) Only a small part of the incident spectrum contributes to each reflection but all of it contributes to the background. Resolution in Laue data sets is therefore lower than resolution in corresponding monochromatic data sets. (ii) Laue exposures contain fewer low resolution reflections[34,35], and as a consequence, motion, disorder, and the shape and extent of the molecular envelope are difficult to describe from Laue measurements. (iii) The Laue geometry is sensitive to the mosaicity of crystals, and crystals with a slightly imperfect lattice make reflections radially elongated. An increase of mosaicity and disorder accompanies most structural transitions in crystals. Not all reactions that take place in crystals are thus suitable for kinetic analysis with the Laue technique. Consequently, most of the biologically significant structural results on reaction intermediates, and practically all structures on native proteins, have come from monochromatic diffraction studies.

Structural rearrangements of cytochrome cd_1

Time-resolved structural studies on cytochrome cd_1 nitrite reductase have led to the proposal that late steps in the folding of a protein may be utilized in structural transitions required for the function of the protein[24]. Cytochrome cd_1 nitrite reductase from *Paracoccus pantotrophus* (formerly known as *Thiosphaera pantotropha*) is a bifunctional enzyme that catalyzes the one-electron reduction of nitrite to nitric oxide ($NO_2^- + 2H^+ + e^- \rightarrow NO + H_2O$), the committed step of denitrification, and the four-electron reduction of oxygen to water ($O_2 + 4H^+ + 4e^- \rightarrow 2H_2O$), which is a cytochrome oxidase reaction. The crystal structure of the oxidized enzyme[36] shows the d_1 heme iron of the active site ligated by His 200/Tyr 25 side chains, and the *c* heme iron by a His 17/His 69 ligand pair.

Time-resolved structural studies on nitrite reduction[24] revealed a fascinating view of the enzyme undergoing major structural rearrangements. Single crystal microspectrophotometry and X-ray crystallography were used to follow the reaction in the crystal. Reaction intermediates were trapped by freeze quenching crystals at ~90 K, and monochromatic data sets were collected to high resolutions from these intermediates. The results show that

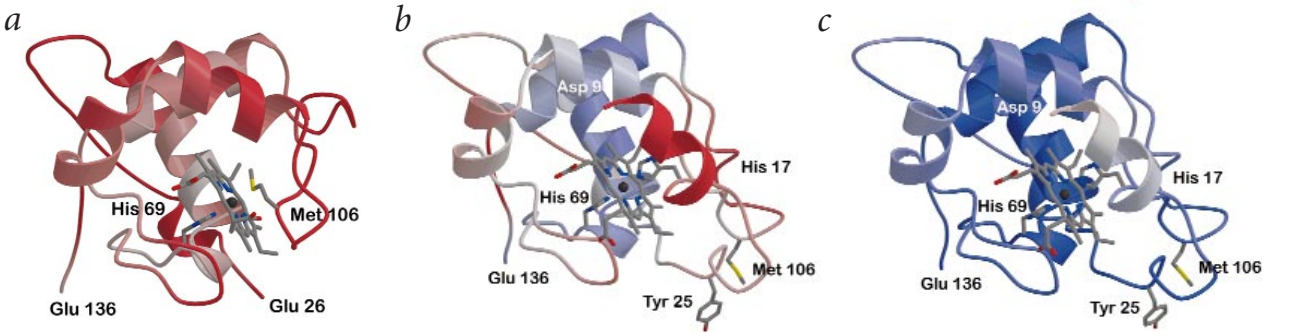

Fig. 1 The *c*-type cytochrome domain of cytochrome cd_1 in three different states[24]. The *c* domain is colour coded according to B-factors (blue: 5 Å^2; red: 40 Å^2). ***a***, Structure of the *c*-domain in the reduced enzyme. ***b***, An intermediate structure during reoxidation with nitrite. ***c***, Structure of the *c*-domain in the oxidized enzyme.

both hemes undergo religation during catalysis. Upon reduction, the tyrosine ligand of the d_1 heme is released to allow substrate binding. Concomitantly, an unexpected refolding of the cytochrome *c* domain takes place, resulting in a change of the *c* heme iron coordination from His 17/His 69 to Met 106/His 69 (Fig. 1). This step is reminiscent of late steps in the folding of cytochrome *c*[37], and raises the intriguing possibility that cytochrome cd_1 utilizes an element of a folding process in its functional cycle[24]. The structural change between oxidized and reduced cytochrome cd_1 shows how redox energy can be converted into conformational energy within a heme protein, a phenomenon that has general importance. Structures of reaction intermediates reveal how nitric oxide is formed and expelled from the active site iron, as well as the return of both hemes to their starting coordination in the crystal. Based on these structures, quantum mechanical (QM) calculations were performed in combination with simulated annealing (SA) and molecular mechanics (MM) to determine the electronic distribution of molecular orbitals in the active site during catalysis[38]. The results show likely trajectories for electrons, protons, substrates and products during nitrite reduction, and offer an interpretation of the reaction mechanism.

Return of Tyr 25 to a hydrogen bonding position between His 345 and His 388 facilitates product release, but rebinding of Tyr 25 to the oxidized iron may be bypassed in steady state catalysis. Recent solution studies by EPR and absorption spectroscopy[39] confirm these conclusions, and show the formation of the catalytically competent form of the enzyme with 'switched' heme axial ligands (Fig. 1*a*). Following oxidation, this structure slowly returns (at 25 °C) to the resting state (Fig. 1*c*), a process that takes ~20 min at 25 °C (ref. 39).

Copper amine oxidase

Oxygen activation is a fundamental process in aerobic biology, and yet it is poorly understood. Recent time-resolved diffraction studies[25] have captured, for the first time, a bound dioxygen species at a copper center (Fig. 2*a*). Ubiquitous copper amine oxidases are extracellular or cell surface enzymes that convert primary amines to aldehydes with the concomitant release of hydrogen peroxide and ammonia (Fig. 2*b*). Copper amine oxidases are linked to medical conditions such as congestive heart diseases or complications in diabetes.

The catalytic mechanism (Fig. 2*b*) involves a two-electron redox reaction with only a single copper at the active site. The second redox site is provided by a novel quinone cofactor, 2,4,5-trihydroxyphenylalanine quinone (TPQ), derived from a constitutive tyrosine (for a review see ref. 40). The reductive half reaction (species 1 → 3, Fig. 2*b*) has been well-characterized biochemically and proceeds *via* Schiff base formation between the TPQ cofactor and an amine substrate. This is followed by hydrolysis of the Schiff base to yield an aldehyde product and a twice reduced quinone cofactor in the form of aminoquinol[40,41] (species 3, Fig. 2*b*). The mechanism of the oxidative half reaction in which molecular oxygen is used to regenerate species 1 has been the subject of intense debate.

Wilmot and coworkers[25] exploited the fact that copper amine oxidase from *E. coli* is fully active in the crystalline state, and the catalytic reaction is accompanied by a rich palette of visible spec-

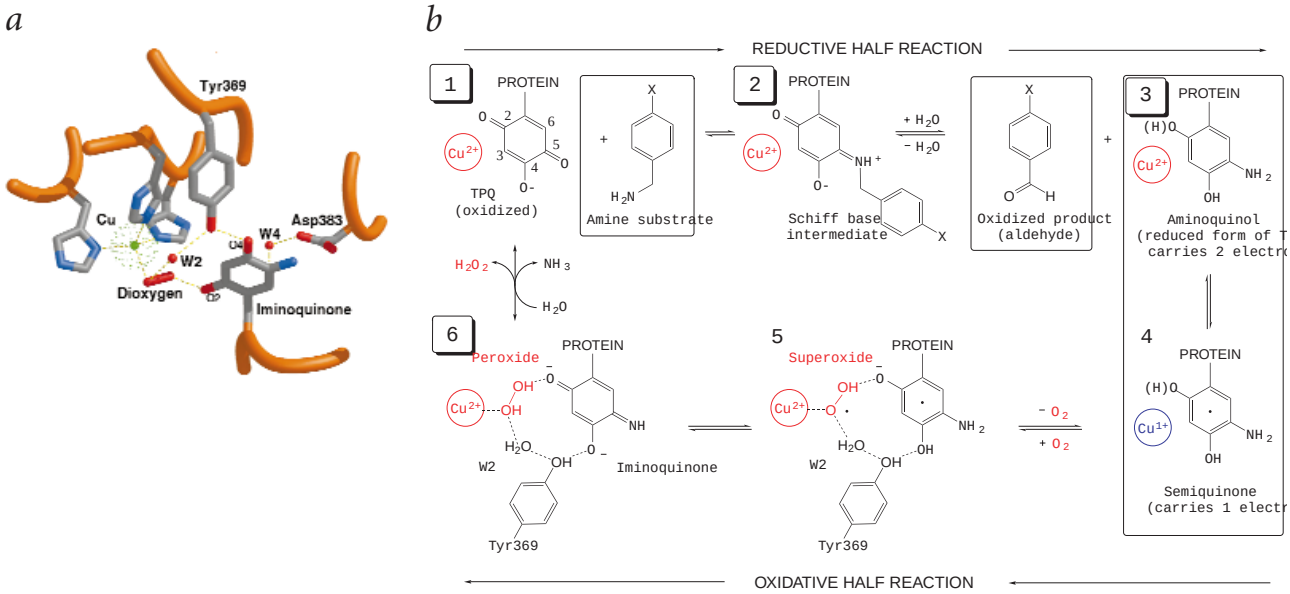

Fig. 2 First view of a bound dioxygen species at a copper center[25]. ***a***, The figure shows the rate-determining intermediate in the active site of *E. coli* amine oxidase. Yellow dashed lines indicate H-bonding and van der Waals interactions. Proton transfer pathways to the bound dioxygen species from the O2 and O4 atoms of the cofactor (shown here in its iminoquinone form) are evident. From the O2 atom of the cofactor direct transfer is possible to one of the oxygen atoms of the dioxygen species, while from the O4 atom a structurally conserved path exists to the other oxygen atom of the dioxygen species, involving the hydroxyl of Tyr 369 and a water molecule (W2). Another water (W4) is poised above the imino group of iminoquinone, suggesting hydrolysis mediated by a conserved aspartic acid (Asp 383) as the route for regeneration of the oxidized cofactor (2,4,5-trihydroxyphenylalanine quinone, TPQ) releasing ammonia. The structure corresponds to species 6 in (*b*). ***b***, The reaction cycle of *E. coli* amine oxidase. The enzyme in the oxidized resting state (species 1, PDB code 1DYU) reacts with the amine substrate to form a Schiff base (species 2, PDB code 1SPU) between the substrate and the cofactor (TPQ). Following hydrolysis of the Schiff base, the product aldehyde is released, leaving a doubly reduced enzyme behind in which the two extra electrons are distributed in an equilibrium between a Cu(II)-aminoquinol species (PDB code 1D6U; species 3) and a Cu(I)-semiquinone species (species 4). The reduced cofactor is reoxidized to TPQ by molecular oxygen probably *via* a semiquinone-Cu^{2+}-superoxide (species 5) to give the product hydrogen peroxide and iminoquinone-Cu^{2+} (species 6, PDB code 1D6Z). Hydrolysis of the iminoquinone would regenerate TPQ or alternatively, attack by the amine substrate would lead to the formation of the substrate Schiff base. Crystal structures[25,41,54] have been obtained for species 1,2,3 and 6. The visible spectrum of semiquinone, either species 4 or 5, is observed during turnover.

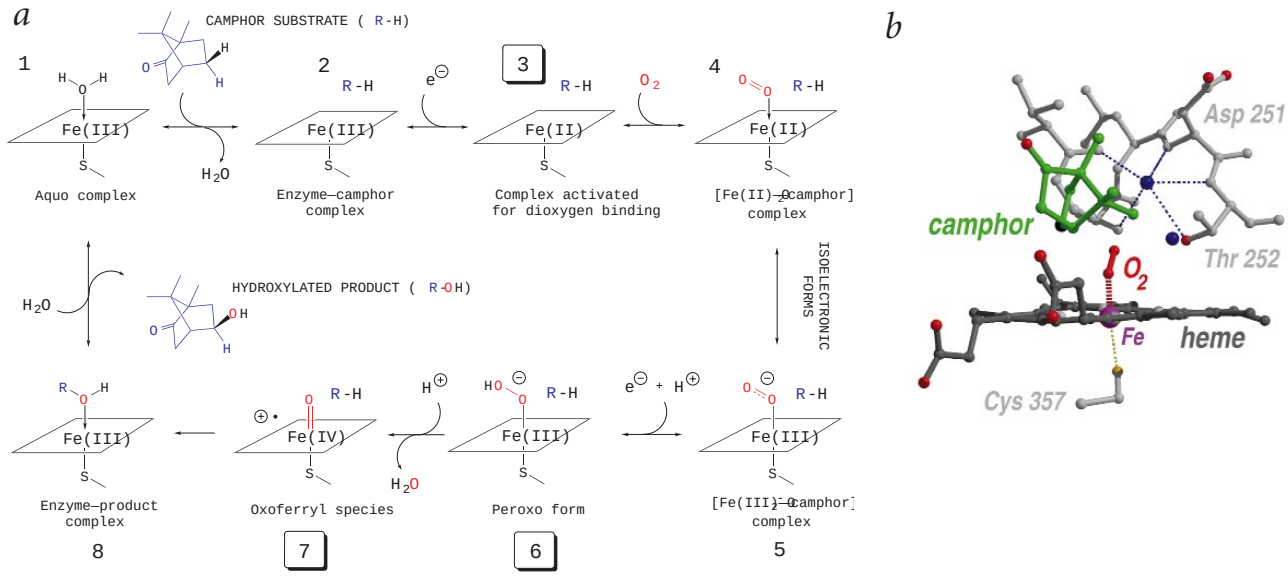

Fig. 3 The reaction cycle of cytochrome P450cam. ***a***, Substrate binding converts the six-coordinate, low-spin form of the protein (species 1) to the five-coordinate, high-spin Fe(III) camphor complex (species 2). Addition of the first electron reduces the enzyme to the five-coordinate Fe(II) camphor complex (species 3). Binding of molecular oxygen gives the six-coordinate Fe(II)–O_2 dioxygen intermediate (species 4) in equilibrium with the six-coordinate Fe(III)-O_2^- intermediate (species 5). Addition of a second electron and two protons results in the cleavage of the oxygen–oxygen bond (species 6,7) to produce a molecule of water and an oxidizing species, the so-called activated oxygen intermediate (species 7). Insertio n of the iron-bound oxygen into the substrate gives the product, 5-exo-hydroxycamphor. Structures for intermediates 3, 6 and 7 have recently been r eported[17]. ***b***, The active site of cytochrome P450cam with a bound dioxygen species[17]. The most likely interpretation of the results is that this structure corresponds to species 6 in (*a*). Two well-ordered water molecules (blue) form hydrogen bonds with the highly conserved Asp 251 and Thr 252, both of which had been implicated in the catalytic reaction. The dioxygen species is in van der Waals contact with the camphor substrate.

tral changes due to the redox changes taking place at the TPQ site. Certain steps of the reaction are dramatically slowed down in the crystal compared to solution, and freeze trapping in liquid nitrogen can be used to halt the reaction at these stages. Most revealing was the 2.1 Å structure of the intermediate accumulated before the rate-determining step, which permitted the direct visualization of dioxygen bound to a mononuclear copper center. The TPQ was in the iminoquinone state (oxidized aminated form), which was a postulated intermediate in the reaction but had never been observed. This observation indicates that the dioxygen species was the product hydrogen peroxide (species 6, Fig. 2*b*), spanning between the copper ion and the O2 position of iminoquinone. The dioxygen species formed a weak side-on interaction with the metal in the complex. The first electron to molecular oxygen could come from either Cu^+ or aminoquinol[42] to give Cu^{2+}, superoxide and the one-electron reduced semiquinone, whose spectrum is observed during turnover in crystals (species 4 or 5, Fig. 2*b*). The second electron would come from the semiquinone to yield the iminoquinone species (species 6, Fig. 2*b*).

Proton transfer pathways from O2 and O4 of the cofactor to dioxygen are suggested by the structure; in the case of O2 by direct transfer and for O4 in a structurally conserved path involving the hydroxyl of a tyrosine and a water molecule. A water molecule is poised above the aminated C5 position of the iminoquinone, suggesting that hydrolysis leading to TPQ and ammonia, is mediated by a conserved aspartic acid (Fig. 2*a*). The time-resolved crystal structure revealed the major features of oxygen activation in this important class of enzymes, and demonstrated the power of freeze trapping techniques in enzymology, particularly when combined with spectroscopy to 'place' the structure along the reaction coordinate.

Intermediates during oxygen activation

Charge exchange reactions between highly oxidized metal centers and neutral molecules play key roles in difficult synthetic and degradative processes in biology. Highly charged metal ions such as Fe(IV) are temporarily created through chemical or photochemical processes in the active sites of some enzymes. Most of these enzymes catalyze reactions that have a very high activation energy barrier, and may require a flame in the laboratory, yet proceed effectively at the active sites of these biological 'blowtorches'[4]. These enzymes play prominent roles in the stereoselective oxidation of inert bonds, such as unactivated carbon–carbon or carbon–hydrogen bonds, and the reactions usually involve radicals. Cytochrome P450cam and isopenicillin N synthase are two such enzymes. They both contain iron, but the iron is present in very different chemical environments in these two enzymes. Cytochrome P450cam is a heme enzyme, while isopenicillin N synthase is a mononuclear ferrous enzyme (the first from this family whose structure could be determined[43]).

Cytochrome P450cam. Members of the cytochrome P450 superfamily catalyze the addition of molecular oxygen to unactivated hydrocarbons at physiological temperature, a reaction that requires high temperature to proceed in the absence of a catalyst. One of the best-characterized enzymes of this family is cytochrome P450cam that catalyzes the stereospecific hydroxylation of camphor to 5-exo-hydroxycamphor (Fig. 3). Structures are available for a number of different forms of this protein (for example, species 1, 2 and 8 in Fig. 3*a*) but the nature of the oxygen-bound species remained unclear. Recent experiments by Schlichting and coworkers[17] revealed structures for three of the key intermediates (species 3, 6 and 7 in Fig. 3*a*). These structures were obtained by trapping techniques and cryocrystallography,

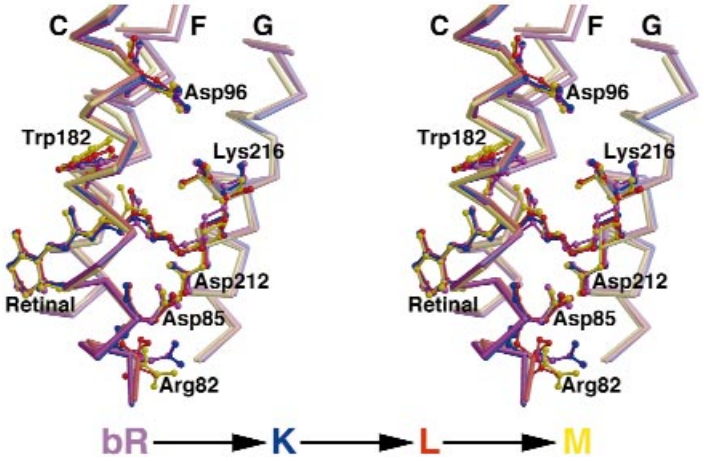

Fig. 4 Light-induced structural changes during the photocycle of bacteriorhodpsins. The ground state model[55] (in purple) is shown with the K[12] (blue), L[15] (red) and M[13] (yellow, D96N mutant) intermediate structures overlaid. Retinal isomerisation from the all *trans* to a 13-*cis* geometry induces a sequence of movements in the surrounding residues. Pronounced movements of the main chain and side chain of Lys 216, which is covalently bound to the retinal through a Schiff base linkage, are visible in all three intermediate structures. Similarly, a movement of Asp 85 towards Asp 212 is prominent in the L-state, but is less pronounced in the M-state. A 'downwards' twist of Arg 82, as well as an 'upwards' movement of Trp 182, become prominent in the M-state. A slight movement of the cytoplasmic side of helix F is apparent in the M-state, although the D96N M-state structure the terminal residues of helices F and G could not be built due to disorder.

and by driving catalysis in frozen crystals using electrons liberated through radiolysis.

To form a bound dioxygen complex, the authors first exposed the enzyme–substrate–Fe(II) complex to high pressures of oxygen. After three minutes in oxygen, the crystals were flash frozen in liquid nitrogen and a data set collected using 0.91 Å wavelength X-rays. At short X-ray wavelengths, only small amounts of photoelectrons are released in the sample during data collection compared to the number released at longer wavelengths. Thus the authors were able to obtain a structure for a bound dioxygen species (Fig. 3*b*) without accidentally driving the catalytic reaction to completion during data collection. Following data collection at 0.91 Å, the same crystal (still frozen at ~96 K) was exposed for three hours to longer wavelength X-rays (1.5 Å) to effect cleavage of the dioxygen species by electrons liberated during radiolysis. Another data set collected at 0.91 Å showed evidence that the reaction proceeded further, and that the dioxygen species was converted to a mono-oxygen species (most likely species 7, Fig. 3*a*, although other possibilities such as either a hydroxide ion or a water molecule bound to the heme iron were also acknowledged). The structures show small but significant conformational changes in several important residues and reveal a network of bound water molecules that may provide the protons needed for the reaction.

Isopenicillin N synthase. Isopenicillin N synthase (IPNS) catalyzes the biosynthesis of a β-lactam compound isopenicillin N (IPN), the precursor of all penicillins and cephalosporins. The key steps in this reaction are the two iron-dioxygen-mediated ring closures of the tripeptide δ-(L-α-aminoadipoyl)-L-cysteinyl-D-valin (ACV). This reaction cannot be performed by heme enzymes such as cytochrome P450. Mononuclear ferrous enzymes have three accessible binding sites around the iron for substrate and dioxygen binding whereas heme enzymes, like cytochromes P450, have only one. As a consequence, mononuclear iron enzymes participate in a far wider range of reactions than conventional heme enzymes. It has been proposed that the peptide substrate and dioxygen bind simultaneously to the iron, and that the four-membered β-lactam ring is formed initially, associated with a highly oxidized Fe(IV)-oxo (ferryl) moiety, which subsequently mediates closure of the five-membered thiazolidine ring.

Burzlaff *et al.*[26] describe observation of the IPNS reaction in crystals by X-ray crystallography. They grew IPNS–$Fe2^{+}$–substrate crystals anaerobically, exposed the crystalline complex to high pressures of oxygen (40 bar) to promote reaction and then froze the crystals in liquid nitrogen. Data were then collected to high resolutions (1.35–1.45 Å) with monochromatic X-rays. No intermediate with bound oxygen could be captured, but using the natural substrate ACV, they were able to trap the labile IPNS–$Fe2^{+}$–IPN product complex, which decomposes through hydrolysis in minutes in solution. With the substrate analog, δ-(L-α-aminoadipoyl)-L-cysteinyl-L-S-methyl-cysteine (ACmC) in the crystal, the reaction cycle was interrupted at the monocyclic stage. These mono- and bicyclic structures support the hypothesis of a two-stage reaction sequence leading to penicillin. Furthermore, the formation of a monocyclic sulfoxide product from ACmC is most simply explained by the involvement of a high valency iron species, although this was not visible in the electron density maps.

Bacteriorhodopsin

Proton pumping across biological membranes is a fundamental process in energy utilization in living organisms. Membrane proteins capable of creating proton gradients belong to two distinct classes of proton pumps: those that use visible light to create a proton gradient, and those that use a chemical process to move protons across a membrane. Bacteriorhodopsin is the simplest known light-driven proton pump and, as such, provides a paradigm for the study of a key mechanism in bioenergetics. The chromophore of bacteriorhodopsin is a retinal molecule that is covalently bound to Lys 216 *via* a protonated Schiff base. Following the absorption of a visible photon the protein passes through a sequence of intermediate states, bR → K ↔ L ↔ M1 → M2 ↔ N ↔ O → bR, which are characterized by distinct spectral features. Recent time-resolved structural studies have provided the first high resolution pictures on events in proton pumping by bacteriorhodopsin (Fig. 4).

The structure of the K intermediate[12] was elucidated by illuminating a crystal cooled to ~110 K. The results show that retinal isomerization moves the backbone carbonyl of Lys 216 by pulling the lysyl side chain *via* the Schiff base linkage. A water molecule (Wat 402), which plays a pivotal role in stabilizing counter ions in the ground state (or bR state), becomes disordered, enabling the carboxylates of Asp 85 and Asp 212 to approach each other. The recent X-ray structure of the L-state intermediate[15] captured at ~170 K shows how the movements observed in the K-state evolve with time. Most strikingly the disordering of Wat 402 induces the collapse of a network of water-mediated hydrogen bonds stretching from the Schiff base to Arg 82 (Fig. 4). This is accompanied by a bending of helix C, allowing Asp 85 (the primary proton accep-

tor) to move into proximity of the protonated Schiff base. Two hydrogen bonds that stabilize the negatively charged Asp 85 in the ground state structure are broken in the L-state, and the only hydrogen bond that remains arises from a reordering of a water molecule, connecting Asp 85 to Asp 212. The mutual approach of the negatively charged carboxylates of Asp 85 and Asp 212 creates an electrostatic environment in which proton transfer from the Schiff base to Asp 85 is facilitated. A relaxation of helix C following proton transfer was suggested as a means for drawing the Schiff base and Asp 85 apart, ensuring the directionality of the overall mechanism. An alternative mechanism assigns a straightening of the retinal as a mechanism for separating these two groups following proton transfer[44].

X-ray structures for the early and late M intermediates were also captured by trapping methods. Structures of the M-state for wild type bacteriorhodopsin[16], the D96N mutant[13], and the E204Q mutant[45] all show a similar rearrangement of water molecules on the extracellular side of the protein as that seen in the L-state. Furthermore, an unwinding of helix G near Ala 215 and Lys 216 is seen to allow the ordering of a series of water molecules in a region which, in the resting state, presents a highly hydrophobic channel. These waters define a proton translocation pathway from Asp 96 toward the isomerized Schiff base (Fig. 4) and explain how the Schiff base accessibility is switched from the extracellular side to the cytoplasmic side during the photocycle. A failure to observe any large scale movements[13,16,45] on the cytoplasmic sides of helices F and G appears in conflict with recent electron crystallography results. A low resolution three-dimensional structure of the F219L mutant tapped in the N-state[46] showed a significant outwards tilt of helix F. A more detailed view of a similar structural change was obtained through higher resolution electron diffraction studies on a triple mutant[44] D96G,F171C,F219L, which adopts the full extent of the light driven conformational change of wild type bacteriorhodopsin in its resting state. Such an opening of the cytoplasmic channel is believed to facilitate the reprotonation of the Schiff base by Asp 96. All structures combined provide a three-dimensional picture of structural transitions in this molecular pump.

New possibilities for data collection

In time-resolved diffraction studies and in some studies of trapped intermediates, multiple structural states are deliberately created in the crystal. It was shown recently[47] that in such mixed crystals additional, independent information can be obtained on the structural changes from X-ray diffraction. The diffraction pattern of a randomly mixed crystal consists of two components. One is the well-known Bragg diffraction pattern of the 'average' crystal, which can be decomposed into the sum of structural states, as discussed above. The other is a continuous (diffuse) diffraction pattern. For a single reacting species, the diffraction pattern represents the 'difference' molecule — that is, the difference between those that have reacted and those that have not. Simulations show that the structure of the 'difference molecule' can be recovered in three dimensions perfectly and without phase uncertainty, by the existing crystallographic program EDEN[48,49].

The diffuse diffraction pattern has several attractive properties. First, it directly measures the interesting parts of the molecule — those that undergo changes. Second, it is quite insensitive to the long range order of the crystal, as opposed to monochromatic and Laue methods. Third, it 'solves the phase problem' by enabling the measurement of the diffraction pattern in between the Bragg peaks — a method called oversampling. Finally, the integrated intensity of the continuous diffraction pattern is comparable to that of the discrete diffraction pattern obtained from monochromatic or Laue methods. On the negative side, the continuous background due to crystal disorder, thermal motion and experimental artifacts will have to be measured separately and subtracted out. Nevertheless, the success of similar methods — X-ray and photoelectron holography (for a review see ref. 50) and recent experiments by Sayre and Miao[51] — give us confidence that careful experiments along these lines will yield unambiguous electron densities of the active parts of molecules.

New possibilities in reaction initiation

Reaction initiation either with photons or by the diffusion of reactants can be a limiting factor in structural kinetics. Time-resolved structural studies on diffusion-triggered processes could be extended to a much wider range of systems if one could lower the diffusion barriers. One obvious possibility for lowering diffusion barriers is to reduce the sample size, and use nanoclusters or nanocrystalline enzyme assemblies of micron or submicron dimensions for time-resolved structural studies. With very small samples, the vast majority of solution techniques and methodologies would become available for time-resolved structural investigations. Emerging X-ray free electron lasers[52,53] could provide hard X-ray flashes with pulse durations of <100 fs and peak brilliance of 10–11 orders of magnitude higher than what is currently available from third generation synchrotrons. Such pulses may allow structural studies on large biomolecules or nanometer scale clusters before the effect of radiation damage destroys the sample[21]. Under these conditions, a new nanocluster/nanocrystal will be needed for each exposure. We foresee that container-free sample-handling methods based on spraying techniques or methods adopted from cryo-electron microscopy, combined with future light source development, will open up new horizons for time-resolved structural studies.

Acknowledgments

This work was supported by the Swedish Research Councils, the EU-Biotech Programme STINT, EMBO and the BBSRC Structural Biology Initiative.

Received 30 August, 2000; accepted 3 October, 2000.

1. Hajdu, J., Acharya, K. R., Barford, D., Stuart, D. I. & Johnson, L. N. Catalysis in enzyme crystals. *Trends Biochem. Sci.* **13**, 104–109 (1988).
2. Hajdu, J. & Andersson, I. Fast crystallography and time-resolved structures. *Annu. Rev. Biophys. Biomol. Struct.* **22**, 467–498 (1993).
3. Schlichting, I. & Goody, R.S. Triggering methods in crystallographic enzyme kinetics. *Methods Enzymol.* **277**, 467–490 (1997).
4. Hadfield, A. T. & Hajdu, J. On the photochemical release of phosphate from 3,5-dinitrophenyl phosphate in a protein crystal. *J. Mol. Biol.* **236**, 995–1000 (1994).
5. Brubaker, M.J., Dyer, D.H., Stoddard, B. & Koshland, D.E. Synthesis, kinetics, and structural studies of a photolabile caged isocitrate: A catalytic trigger for isocitrate dehydrogenase. *Biochemistry* **35**, 2854–2864 (1996).
6. Schlichting, I., Berendzen, J., Phillips, G.N. & Sweet, R.M. Crystal-structure of photolyzed carbonmonoxy-myoglobin. *Nature*, **371**, 808–812 (1994).
7. Srajer, V. *et al.* Photolysis of the carbon-monoxide complex of myoglobin - nanosecond time-resolved crystallography. *Science* **274**, 1726–1729 (1996).
8. Genick, U.K. *et al.* Structure of a protein photocycle intermediate by millisecond time-resolved crystallography. *Science* **275**, 1471–1475 (1997).
9. Genick, U.K., Soltis, S.M., Kuhn, P., Canestrelli, I.L. & Getzoff, E.D. Structure at 0.85 Angstrom resolution of an early protein photocycle intermediate. *Nature* **392**, 206–209 (1998).
10. Stoddard, B.L. New results using Laue diffraction and time-resolved crystallography. *Curr. Opin. Struct. Biol.* **8**, 612–618 (1998).
11. Perman, B. *et al.* Energy transduction on the nanosecond time scale: Early structural events in a xanthopsin photocycle. *Science* **279**, 1946–1950 (1998).
12. Edman, K. *et al.* High-resolution X-ray structure of an early intermediate in the bacteriorhodopsin photocycle. *Nature*, **401**, 822–826 (1999).
13. Luecke, H., Schobert, B., Richter, H.T., Cartailler, J.P. & Lanyi, J.K. Structural changes in bacteriorhodopsin during ion transport at 2 Angstrom resolution. *Science* **286**, 255–260 (1999).
14. Chu, K. *et al.* Structure of a ligand-binding intermediate in wild-type carbonmonoxy myoglobin. *Nature* **403**, 921–923 (2000).
15. Royant, A. *et al.* Helix deformation is coupled to vectorial proton transport in the photocycle of bacteriorhodopsin. *Nature* **406**, 645–648 (2000).
16. Sass, H. J. *et al.* Structural alterations for proton translocation in the M state of wild type bacteriorhodopsin. *Nature* **406**, 649–653 (2000).
17. Schlichting, I. *et al.* The catalytic pathway of cytochrome P450cam at atomic resolution. *Science* **287**, 1615–1622 (2000).
18. Larsson, J. *et al*. Ultrafast structural changes measured by time-resolved X-ray diffraction. *App. Phys. A* **66**, 587–591 (1998).
19. Rischel, C. *et al.* Femtosecond time-resolved X-ray diffraction from laser-heated organic films. *Nature* **390**, 490–492 (1997).
20. Neutze, R. & Hajdu, J. Femtosecond time resolution in X-ray diffraction experiments. *Proc. Natl. Acad. Sci. USA*. **94**, 5651–5655 (1997).
21. Neutze, R., Wouts, R., van der Spoel, D., Weckert & E. Hajdu, J. Potential for femtosecond imaging of biomolecules with X-rays. *Nature* **406**, 752–757 (2000).
22 Zewail, A.H., Femtochemistry: Atomic-scale dynamics of the chemical bond. *J. Phys. Chem.* **A104**, 5660–5694 (2000).
23. Gouet, P *et al.* Ferryl intermediates of catalase captured by time-resolved Weissenberg crystallography and UV-VIS spectroscopy. *Nature Struct. Biol.* **3**, 951–956 (1996).
24. Williams, P.A. *et al.* Heme ligand-switching during catalysis in crystals of a nitrogen cycle enzyme. *Nature*, **389**, 406–412 (1997).
25. Wilmot, C.M., Hajdu, J., McPherson, M.J., Knowles, P.F. & Phillips, S.E.V., Direct visualisation of dioxygen bound to a mononuclear copper centre during enzyme catalysis. *Science* **286**, 1724–1728 (1999).
26. Burzlaff, N.I *et al.* The reaction cycle of isopenicillin N synthase observed by X-ray diffraction. *Nature* **401**, 721–724 (1999).
27. Hajdu, J. *et al.* Catalysis in the crystal: Synchrotron radiation studies with glycogen phosphorylase b. *EMBO J.* **6**, 539–546 (1987).
28. Hajdu, J. *et al.* Millisecond X-ray diffraction: First electron density map from Laue photographs of a protein crystal. *Nature* **329**, 178–181(1987).
29. Fülöp, V. *et al*. Laue diffraction study on the structure of cytochrome *c* peroxidase compound I. *Structure* **2**, 201–208 (1994).
30. Moffat, K. Time-resolved crystallography. *Acta Crystallogr. A* **54**, 833–841 (1998).
31. Hadfield, A. T. & Hajdu, J. A fast and portable micro-spectrophotometer for time-resolved X-ray diffraction experiments. *J. Appl. Crystallogr.* **26**, 839–842 (1993).
32. Mozzarelli, A. & Rossi, G.L. Protein function in the crystal. *Annu. Rev. Biophys. Biomol. Struct.* **25**, 343–365 (1996).
33. Ren, Z. *et al.* Laue crystallography: coming of age. *J. Synchrotron Rad.* **6**, 891–917 (1999).
34. Cruickshank, D. W. J., Helliwell, J. R. & Moffat, K. Multiplicity distribution of reflections in Laue diffraction. *Acta Crystallogr. A* **43**, 656–674 (1987).
35. Clifton, I. J., Elder, M. & Hajdu, J. Experimental strategies in Laue crystallography. *J. Appl. Crystallogr.* **24**, 267–277 (1991).
36. Fülöp, V., Moir, J. W. B., Ferguson, S. J. & Hajdu, J. The anatomy of a bifunctional enzyme: structural basis for reduction of oxygen to water and synthesis of nitric oxide by cytochrome cd_1. *Cell* **81**, 369–377 (1995).
37. Elove, G. A., Bhuyan, A. K. & Roder, H., Kinetic mechanism of cytochrome-c folding - involvement of the heme and its ligands. *Biochemistry* **33**, 6925–6935 (1994).
38. Ranghino, G. *et al.* Quantum mechanical interpretation of nitrite reduction by cytochrome cd_1 nitrite reductase from Paracoccus pantotrophus. *Biochemistry* **39**, 10958–10966 (2000).
39. Allen, J.W.A., Watmough, N.J. & Ferguson, S.J., A switch in heme axial ligation prepares *Paracoccus pantotrophus* cytochrome cd_1 for catalysis, *Nature Struct. Biol.* **7**, 885–888 (2000).
40. Klinman, J.P. Mechanisms whereby mononuclear copper proteins functionalize organic substrates. *Chem. Rev.* **96**, 2541–2561 (1996)
41. Wilmot C.M. *et al.* The catalytic mechanism of the quinoenzyme amine oxidase from Escherichia coli: Exploring the reductive half-reaction. *Biochemistry* **36**, 1608–1620 (1997).
42. Su, Q. & Klinman, J.P., Probing the mechanism of proton coupled electron transfer to dioxygen: the oxidative half-reaction of bovine serum amine oxidase. *Biochemistry* **37**, 12513–12525 (1998).
43. Roach, P. L. *et al.* The crystal structure of isopenicillin N synthase, first of a new structural family of enzymes. *Nature*, **375**, 700–704 (1995).
44. Subramanian, S & Henderson, R. Molecular mechanism of vectorial proton translocation by bacteriorhodopsin. *Nature* **406**, 653–657 (2000).
45. Luecke, H. *et al.* Coupling photoisomerisation of retinal to directional transport in bacteriorhodopsin. *J. Mol. Biol.* **300**, 1237–1255 (2000).
46. Vonk, J. Structure of the bacteriorhodopsin mutant F219L N intermediate revealed by electron crystallography. *EMBO J.* **19**, 2152–2160 (2000).
47. Szöke, A. Time-resolved holographic diffraction at atomic resolution. *Chem. Phys. Lett.* **313**, 777–788 (1999).
48. Szöke, A. Holographic methods in X-ray crystallography. 2. Detailed theory and connection to other methods of crystallography. *Act. Crystallogr. A* **49**, 853–866 (1993).
49. Somoza, J.R. *et al.* Holographic methods in X-ray crystallography 4. A fast algorithm and its application to macromolecular crystallography. *Acta Crystallogr. A* **51**, 691–708 (1995).
50. Faigel, G. & Tegze, M. X-ray holography. *Rep. Progr. Phys.* **62**, 355–393 (1999).
51. Miao, J. W., Charalambous, P., Kirz, J. & Sayre, D. Extending the methodology of X-ray crystallography to allow imaging of micrometre-sized non-crystalline specimens. *Nature* **400**, 342–344 (1999).
52. Winick, H., The linac coherent light source (LCLS): A fourth-generation light source using the SLAC linac. *J. Elec. Spec. Rel. Phenom.* **75**, 1–8 (1995).
53. Wiik, B. H. The TESLA project: an accelerator facility for basic science. *Nucl. Inst. Meth. Phys. Res.* **B398**, 1–8 (1997).
54. Parsons M.R. *et al.* Crystal structure of a quinoenzyme: copper amine oxidase of *Escherichia coli* at 2 Å resolution. *Structure* **3**, 1171–1184 (1995).
55. Belrhali *et al*., Protein, lipid and water organization in bacteriorhodopsin crystals: a molecular view of the purple membrane at 1.9 Å resolution. *Structure* **7**, 909–917 (1999).